Fresnel Equations and Electromagnetic Boundary Conditions Lab Report

Jon Betti, Paul Maldonado, Rahma Tayyab

I. Abstract

This lab report discusses Fresnel Equation effects with elementary boundary conditions. Specifically it deals with uncovering the index of refraction, the critical angle, and Brewster's angle for two different unknown samples. This was done using a laser, a lens, a polarizer, and a power meter connected to a photodetector. The index of refraction was found to be 2.34 for glass and 1.62 for plastic. The critical angle was found to be 25.34 degrees for the glass and 38.24 degrees for plastic. Brewster's angle was found to be 31.76 degrees for plastic to air, 23.17 degrees for glass to air, 58.24 degrees for air to plastic, and 66.83 degrees for air to glass.

II. Introduction

This lab deals experimentally tests Fresnel equations in the case of elementary boundary conditions applied to a transparent, non-magnetic, non-conducting medium. Fresnel equations can briefly be described as equations that describe the fraction of light transmitted and reflected when passing through a medium with a different refractive index. The transmission and reflection of light is analyzed with respect to the case of S-polarized light, or perpendicular light, and P-polarized, or parallel polarized, light (Figure 1).

Figure 1

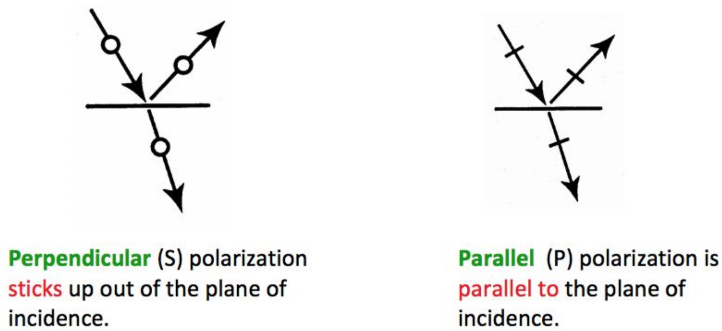

Figure 1: A depiction of S and P polarized light incident on a plane.

The Fresnel equations for perpendicularly polarized light are listed in Eq 1-2 which follow Figure 2. These are similar to the equations for parallel polarized, but are just replaced with $r_{\|}$ and $t_{\|}$. This follows Figure 3.

$$r_{\perp} = \frac{E_{0r}}{E_{0i}} = \frac{n_i cos(\theta_i) - n_t cos(\theta_t)}{n_i cos(\theta_i) + n_t cos(\theta_t)} \quad \text{(Eq 1)}$$

$$t_{\perp} = \frac{E_{0t}}{E_{0i}} = \frac{2 n_i cos(\theta_i)}{n_i cos(\theta_i) + n_t cos(\theta_t)} \quad \text{(Eq 2)}$$

Figure 2

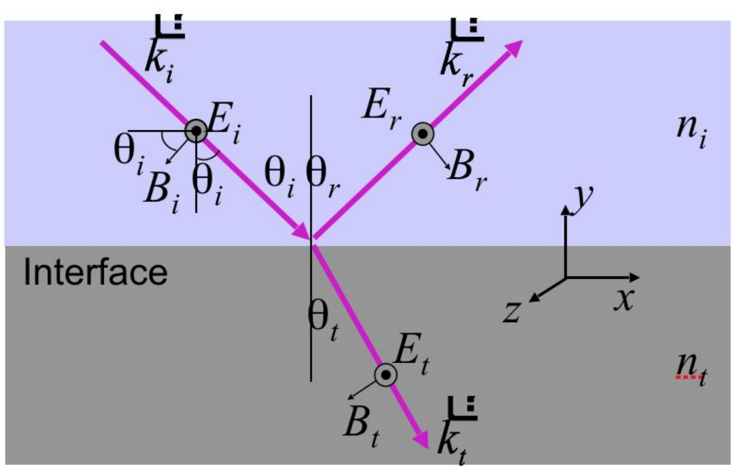

Figure 2: Depiction of boundary and conditions for Fresnel Equations for perpendicularly polarized light.

Figure 3

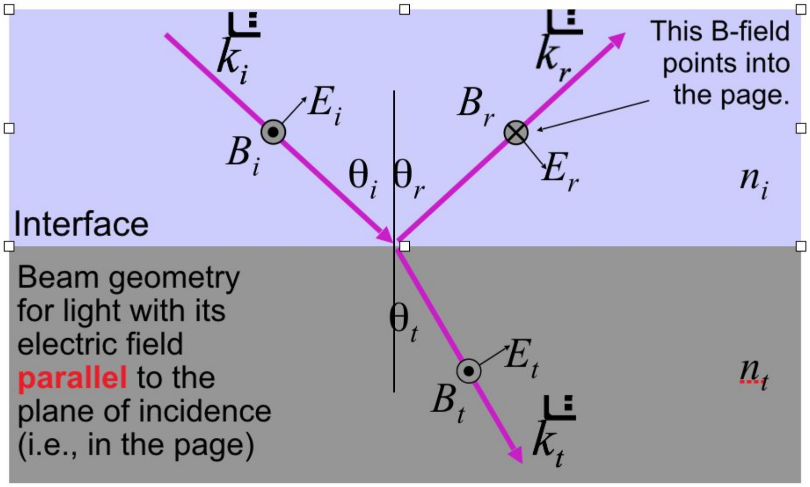

Figure 3: A depiction of the boundary to establish Fresnel equations for parallel polarized light.

This labs also seeks to discover the unknown incidence of refraction of two samples through an analysis of the critical angle along with an analysis of Brewster's angle and its effects. These effects can be analyzed through the use of Snell's law (Eq 3) where n is the index of refraction and θ is the angle with respect to the normal as following either Figure 2 or Figure 3 above.

$$n_i sin(\theta_i) = n_t sin(\theta_t) \qquad \textit{(Eq 3)}$$

III. Apparatus

The apparatus used involved a PASCO setup that includes in order from right to left: a 650nm diode laser, a polarizer, a primary lens, a goniometer with placing for a sample, and a screen with sample hole for a photodetector that is connected to a wattmeter. All degree measurements have a standard deviation of 0.5 degrees and all power measurements have a standard deviation of 5 microwatts or 5 nanowatts, corresponding to the likewise measurement recording.

IV. Data

1. *Initial Observation*

The apparatus was initially changed to attempt to understand at which point the critical angle and Brewster's angle would be able to be determined. Theoretically, the critical angle was figured out to be apparent only in the case of $n_1 > n_2$ as evident by Snell's law (Eq 3). This would then be observed when the transmitted ray would no longer be observable beyond the flat edge of the sample as depicted in Figure 4.

Figure 4

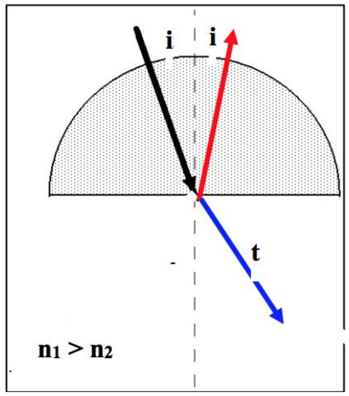

Figure 4: Depiction of light rays incident on a medium that has a larger index of refraction than the medium through which light is originating.

Using the power meter to determine the angle at which the power of the beam dropped significantly from microwatt measurements to nanowatt measurements, the critical angle for both the glass and plastic samples was determined to be approximately 45 degrees $45 \pm 0.5^{\circ}$.

It was theoretically determined using Snell's law (Eq 3) that Brewster's angle could be determined as the point at which vertically polarized light would no longer have an apparent reflected beam, which we measured as approximately 36 degrees.. Data was collected as recorded in Tables 1.1 and 1.2 for predicted angle.

Table 1.1: Plastic Sample

Polarization Angle	Incident Angle	Reflected Angle	Reflected Power	Transmitted Angle	Transmitted Power
90°	36°	76°	400 nW	16°	32 μW
0°	36°	76°	31.8 μW	16°	465 μW

Table 1: Recorded values of power for reflected and transmitted power for a plastic sample where the polarization was varied from vertical at 90 degrees to horizontal at 0 degrees.

Table 1.2: Glass Sample

Polarization Angle	Incident Angle	Reflected Angle	Reflected Power	Transmitted Angle	Transmitted Power
0°	39°	77°	22.4 μW	16°	215 μW
90°	39°	77°	464 nW	16°	15.5 μW

Table 2: Recorded values of power for reflected and transmitted power for a glass sample where the polarization was varied from vertical at 90 degrees to horizontal at 0 degrees.

The results in these tables show that the reflected and transmitted powers show conservation of energy through the transmitted and reflected beams.

2. *Snell's Law*

The angle of the incident beam and refracted beams was recorded for each kind of interface exchange: Air to glass (Table 2.1/Graph 2.1), Glass to Air (Table 2.2/Graph 2.2), Air to Plastic (Table 2.3/Graph 2.3), and Plastic to Air (Table 2.4/Graph 2.4), These were graphed as $sin(\theta_i)$ vs $sin(\theta_t)$ to determine n_{glass}/n_{air} as well as $n_{plastic}/n_{air}$.

Table 2.1: Air to Glass Interface

Incident Angle	Transmitted Angle
15°	6°
20°	9°
25°	10°
35°	14°
40°	16°

Table 2.1: Depicts incident angles vs transmitted angles for air to glass interface.

Graph 2.1: Air to Glass Interface

Graph 2.1: Graphs $sin(\theta_t)$ vs $sin(\theta_i)$ *to obtain a slope of* n_{air}/n_{glass}.

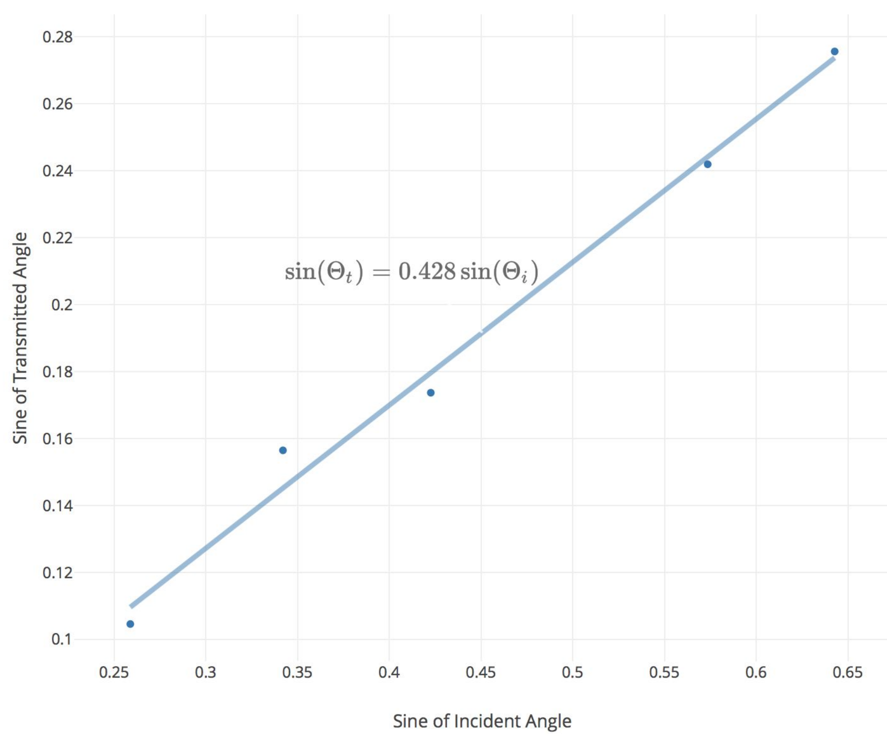

Table 2.2: Glass to Air Interface

Incident Angle	Transmitted Angle
15°	22°
20°	28°
22°	32°
25°	36°
28°	43°

Table 2.2: Depicts incident angles vs transmitted angles for glass to air interface.

Graph 2.2: Glass to AIr Interface

Graph 2.1: Graphs $sin(\theta_t)$ vs $sin(\theta_i)$ *to obtain a slope of* n_{glass}/n_{air}.

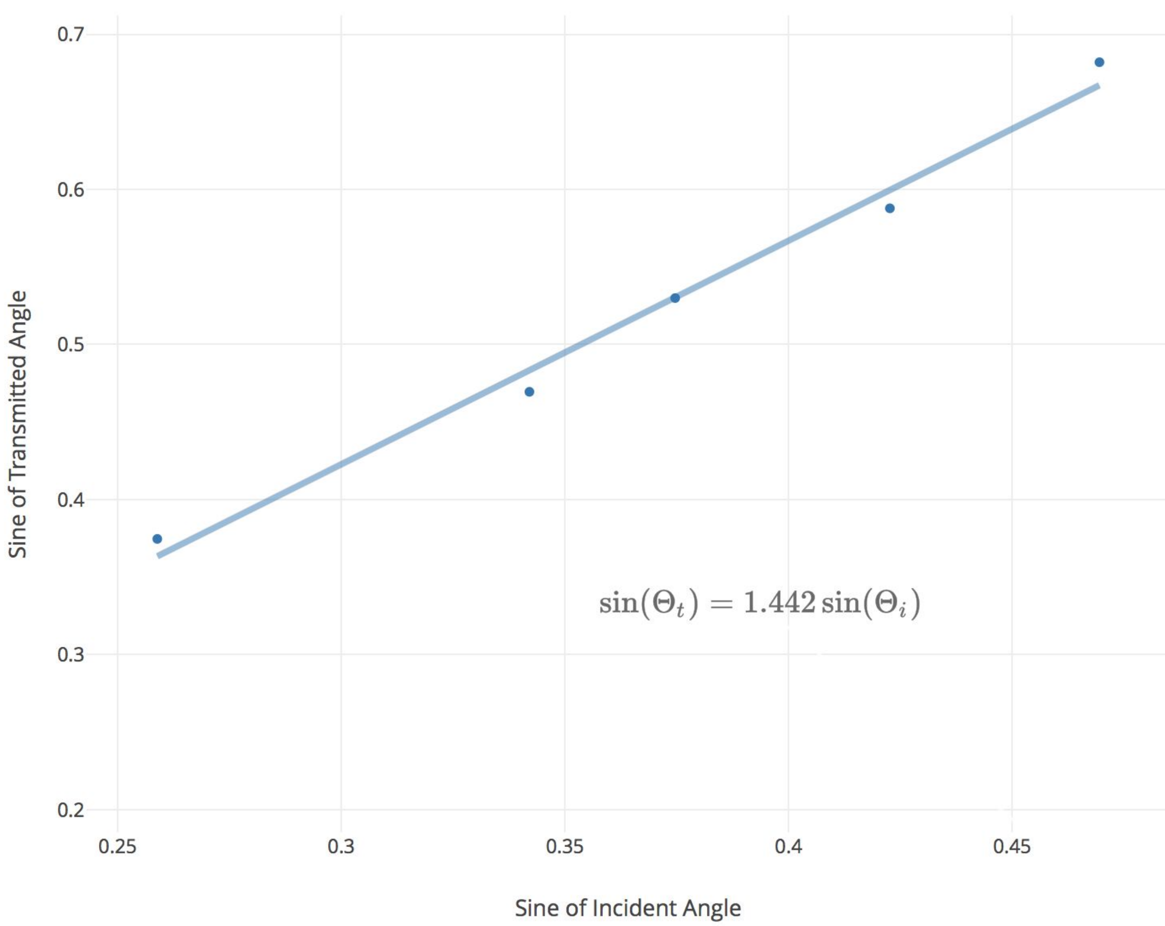

Table 2.3: Air to Plastic Interface

Incident Angle	Transmitted Angle
15°	10°
20°	12°
25°	16°
30°	19°
35°	21°

Table 2.3: Depicts incident angles vs transmitted angles for air to plastic interface.

Graph 2.3: Air to Plastic Interface

Graph 2.3: Graphs $sin(\theta_t)$ vs $sin(\theta_i)$ *to obtain a slope of* $n_{air}/n_{plastic}$.

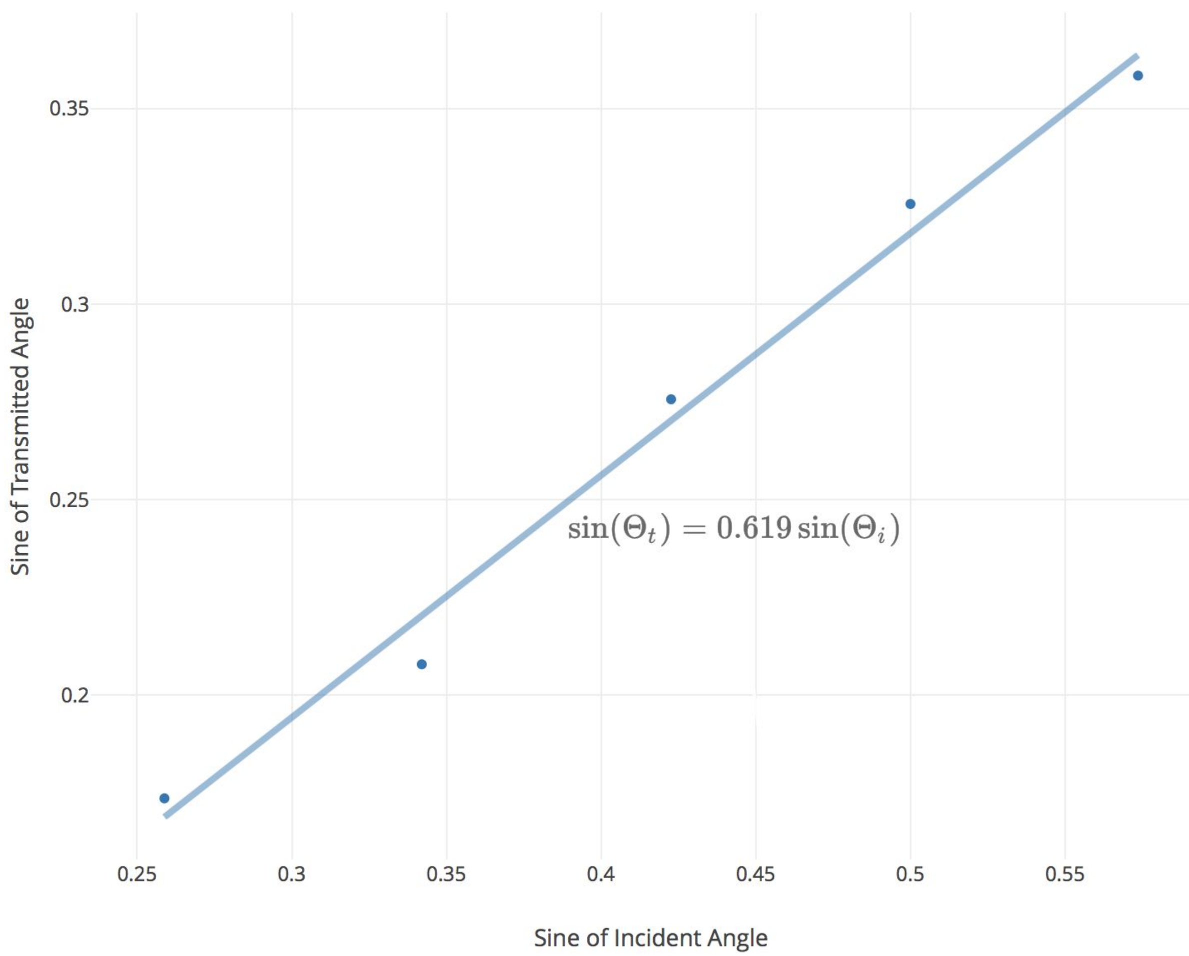

Table 2.4: Plastic to Air Interface

Incident Angle	Transmitted Angle
15°	23°
20°	29°
21°	31°
25°	40°
30°	48°

Table 2.4: Depicts incident angles vs transmitted angles for plastic to air interface.

Graph 2.1: Plastic to Air Interface

Graph 2.1: Graphs $sin(\theta_t)$ vs $sin(\theta_i)$ *to obtain a slope of* $n_{plastic}/n_{air}$.

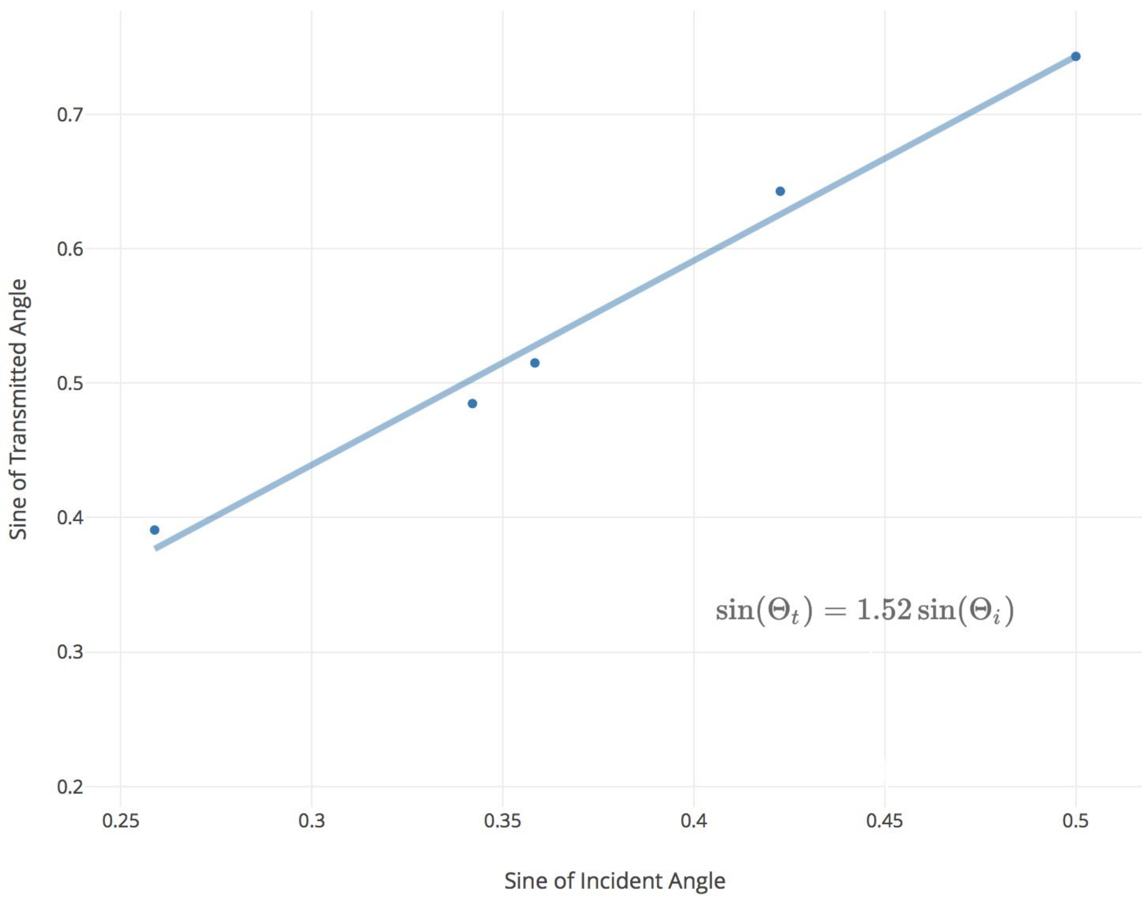

From this our value for the **critical angle of glass** is about **25.34 degrees**

Also our value for the **critical angle of the plastic** is about **38.24 degrees**

These values are clearly different from our initial estimate, which involved visually finding the angle. At that point we had probably messed up measuring the proper angle as we were only looking at the power and the apparatus was less familiar.

3. *Brewster's Angle and Fresnel Equations for Air/Dielectric Interface ($n_2 > n_1$)*

This part of the experiment used the air to glass interface and air to plastic interface and recorded the reflected angle, the refracted angle, the power of the reflected beam, and the power of the transmitted beam for both perpendicular and parallel polarized light (Tables 3.1-3.4). To understand the power measurement, the initial recording was measured without a sample in place and was found to be:

Incident power (p polarization): 39.6 μW
Incident power (s polarization): 593 μW
Incident power (maximum): 615 μW

Table 3.1: Air to Glass Interface (s-polarization)

Incident Angle	Reflected Angle	Reflected Power	Transmitted Angle	Transmitted Power
25°	25°	24.5 μW	16°	254 μW
30°	30°	27.2 μW	20°	259 μW
35°	35°	31.1 μW	23°	250 μW
40°	40°	38.0 μW	24°	246 μW
45°	45°	44.7 μW	28°	245 μW
50°	50°	57.1 μW	30°	246 μW
55°	55°	72.0 μW	33°	232 μW
55°	55°	72.0 μW	33°	232 μW
60°	60°	93.5 μW	34°	221 μW
65°	65°	127 μW	36°	212 μW

70°	70°	168 μW	38°	159 μW

Table 3.1: Recorded raw values for angle and corresponding power for air to glass using perpendicular polarized light.

Table 3.2: Air to Glass Interface (p-polarization)

Incident Angle	Reflected Angle	Reflected Power	Transmitted Angle	Transmitted Power
25°	25°	1.00 μW	19°	35.3 μW
30°	30°	880 nW	22°	35.0 μW
35°	35°	677 nW	25°	35.0 μW
40°	40°	502 nW	27°	35.0 μW
45°	45°	326 nW	32°	34.8 μW
50°	50°	63 nW	33°	35.1 μW
55°	55°	63 nW	36°	35.4 μW
57°	57°	63 nW	36°	35.2 μW
60°	60°	63 nW	37°	35.0 μW
65°	65°	600 nW	38°	34.1 μW

Table 3.2: Recorded raw values for angle and corresponding power for air to glass using parallel polarized light.

Table 3.3: Air to Plastic Interface (s-polarization)

Incident Angle	Reflected Angle	Reflected Power	Transmitted Angle	Transmitted Power
25°	25°	24.5 μW	17°	480 μW
30°	30°	27.7 μW	21°	468 μW
35°	35°	31.9 μW	23°	467 μW
40°	40°	39.2 μW	26°	464 μW

45°	45°	47.5 μW	28°	451 μW
50°	50°	60.0 μW	31°	430 μW
55°	55°	75.2 μW	33°	418 μW
57°	57°	83.3 μW	33°	410 μW
60°	60°	97.1 μW	34°	390 μW
65°		127 μW	37°	355 μW

Table 3.3: Recorded raw values for angle and corresponding power for air to plastic using perpendicular polarized light.

Table 3.4: Air to Plastic Interface (p-polarization)

Incident Angle	Reflected Angle	Reflected Power	Transmitted Angle	Transmitted Power
25°	25°	1.00 μW	19°	35.3 μW
30°	30°	880 nW	22°	35.0 μW
35°	35°	677 nW	25°	35.0 μW
40°	40°	502 nW	27°	35.0 μW
45°	45°	326 nW	32°	34.8 μW
50°	50°	63 nW	33°	35.1 μW
55°	55°	63 nW	36°	35.4 μW
57°	57°	63 nW	36°	35.2 μW
60°	60°	63 nW	37°	35.0 μW
65°	65°	600 nW	38°	34.1 μW

Table 3.4: Recorded raw values for angle and corresponding power for air to plastic using parallel polarized light.

4. Brewster's Angle, Total Internal Reflection and Fresnel Equations for Dielectric/Air Interface ($n_1 > n_2$)

The steps in Part 3 were repeated with glass to air interfaces. In this situation total internal reflection is possible. Recorded values can be found in Tables 4.1-4.2.

Table 4.1 Glass to Air Interface (s-polarization)

Incident Angle	Reflected Angle	Reflected Power	Transmitted Angle	Transmitted Power
25°	25°	6.84 μW	40°	232 μW
29°	29°	2.32 μW	45°	225 μW
30°	30°	7.67 μW	48°	218 μW
32°	32°	12.3 μW	54°	212 μW
34°	34°	14.3 μW	57°	186 μW
35°	35°	17.8 μW	61°	191 μW
37°	37°	22.5 μW	67°	142 μW
40°	40°	41.7 μW	80°	80.6 μW
41°	41°	91.7 μW	77°	1.18 μW
45°	45°	64.8 μW	gone	gone

Table 4.1 Recorded raw values for angle and corresponding power for glass to air using perpendicular polarized light.

Table 4.2: Glass to Air Interface (p-polarization)

Incident Angle	Reflected Angle	Reflected Power	Transmitted Angle	Transmitted Power
25°	25°	63 nW	37°	16.3 μW
29°	29°	63 nW	45°	16 μW
30°	30°	63 nW	49°	16 μW
32°	32°	63 nW	51°	15.9 μW
34°	34°	63 nW	55°	16.2 μW

35°	35°	63 nW	58°	16 μW
37°	37°	116 nW	63°	15.7 μW
40°	40°	500 nW	73°	13.9 μW
41°	41°	5.8 μW	gone	gone
45°	45°	6.09 μW	gone	gone

Table 4.2: Recorded raw values for angle and corresponding power for glass to air using parallel polarized light.

According to the data, it is clear that the polarization of light does not affect the critical angle. It is possible that in 4.1 there is still a result for a transmitted beam at 41 degrees vs. 4.2, but this could be due to an error in the apparatus. It is clear that there is a large dip in power either way at this point. Furthermore, at 45 degrees, which was the estimation of the critical angle from Part 1, both 4.1 and 4.2 with different polarizations show the same results of a undetectable transmitted beam.

From our data we know approximate:
Brewster angle from glass to air is 23.17 degrees
Brewster angle from plastic to air is 31.76 degrees
Brewster angle from air to glass is 66.83 degrees
Brewster angle from air to plastic is 58.24 degrees

Our values once again diverge heavily from our initial estimates not surprisingly because we were very unsure of our measuring techniques in the beginning. Keep in mind error is introduced as we take power measurements because of the diffuse reflection of the laser as it hits the detector. This allows light to scatter as it is reflected instead of a perfect reflection. This causes slight shifts in energy from a perfect reflector.

V. Discussion and Conclusion

From our results we have clearly determined the index of refractions of the two different medium and have found the critical angle and brewster's angle for both. Though our initial predictions were off, looking back after taking data, we did find the angles to agree with our calculated angles from the data, hence our data is accurate and did in fact verify our use of the Fresnel Equations to check the background conditions. If the trial could be done again, we would take more initial measurements to better have a better solid initial prediction, then take more angle measurements at smaller intervals. Of course having a fancier laser, or having an automated way of changing angles would reduce much error as well. In the end changing the dials by hand was a great source of errors, and it took us a little while before we were confident in our readouts. Thus our predictions for part one were inaccurate, but our other measurements are viable.

VI. Bibliography

- Elementary Boundary Conditions on Physics 389 website
- Background Information on Physics 389 website